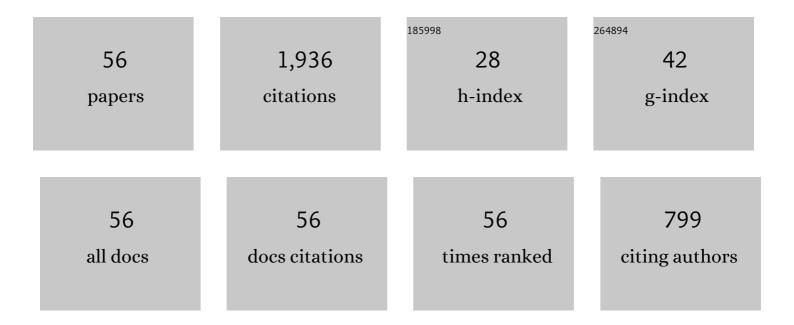
Basem Ahmed Zoheir

List of Publications by Year in descending order

Source: https://exaly.com/author-pdf/8039453/publications.pdf

Version: 2024-02-01



#	Article	IF	CITATIONS
1	New SIMS zircon U-Pb ages and oxygen isotope data for ophiolite nappes in the Eastern Desert of Egypt: Implications for Gondwana assembly. Gondwana Research, 2022, 105, 450-467.	3.0	10
2	Origin of the Volcanic-Arc Signature in Late-Orogenic Granitoids from the Arabian–Nubian Shield. Regional Geology Reviews, 2021, , 439-450.	1.2	0
3	Editorial for the Special Issue: Multispectral and Hyperspectral Remote Sensing Data for Mineral Exploration and Environmental Monitoring of Mined Areas. Remote Sensing, 2021, 13, 519.	1.8	36
4	Hybrid granite magmatism during orogenic collapse in the Eastern Desert of Egypt: Inferences from whole-rock geochemistry and zircon U–Pb–Hf isotopes. Precambrian Research, 2021, 354, 106044.	1.2	20
5	Shear-Related Gold Ores in the Wadi Hodein Shear Belt, South Eastern Desert of Egypt: Analysis of Remote Sensing, Field and Structural Data. Minerals (Basel, Switzerland), 2021, 11, 474.	0.8	35
6	Geochemical and geochronological characteristics of the Um Rus granite intrusion and associated gold deposit, Eastern Desert, Egypt. Geoscience Frontiers, 2020, 11, 325-345.	4.3	18
7	Extreme fractionation and magmatic–hydrothermal transition in the formation of the Abu Dabbab rare-metal granite, Eastern Desert, Egypt. Lithos, 2020, 352-353, 105329.	0.6	18
8	ASTER mapping and geochemical analysis of chromitite bodies in the Abu Dahr ophiolites, South Eastern Desert, Egypt. Arabian Journal of Geosciences, 2020, 13, 1.	0.6	4
9	Phase equilibria, thermodynamic properties, and solubility of quartz in saline-aqueous-carbonic fluids: Application to orogenic and intrusion-related gold deposits. Geochimica Et Cosmochimica Acta, 2020, 283, 201-221.	1.6	25
10	Identifying high potential zones of gold mineralization in a sub-tropical region using Landsat-8 and ASTER remote sensing data: A case study of the Ngoura-Colomines goldfield, eastern Cameroon. Ore Geology Reviews, 2020, 122, 103530.	1.1	83
11	Application of Landsat-8, Sentinel-2, ASTER and WorldView-3 Spectral Imagery for Exploration of Carbonate-Hosted Pb-Zn Deposits in the Central Iranian Terrane (CIT). Remote Sensing, 2020, 12, 1239.	1.8	89
12	Mineral Resources in Egypt (I): Metallic Ores. Regional Geology Reviews, 2020, , 521-587.	1.2	8
13	Multispectral and Radar Data for the Setting of Gold Mineralization in the South Eastern Desert, Egypt. Remote Sensing, 2019, 11, 1450.	1.8	52
14	Mapping Listvenite Occurrences in the Damage Zones of Northern Victoria Land, Antarctica Using ASTER Satellite Remote Sensing Data. Remote Sensing, 2019, 11, 1408.	1.8	60
15	Field and spaceborne imagery data for evaluation of the paleo-stress regime during formation of the Jurassic dike swarms in the Kalateh Alaeddin Mountain area, Shahrood, north Iran. Arabian Journal of Geosciences, 2019, 12, 1.	0.6	6
16	Orogenic Gold in Transpression and Transtension Zones: Field and Remote Sensing Studies of the Barramiya–Mueilha Sector, Egypt. Remote Sensing, 2019, 11, 2122.	1.8	70
17	Mapping hydrothermal alteration zones and lineaments associated with orogenic gold mineralization using ASTER data: A case study from the Sanandaj-Sirjan Zone, Iran. Advances in Space Research, 2019, 63, 3315-3332.	1.2	92
18	Orogenic gold in the Egyptian Eastern Desert: Widespread gold mineralization in the late stages of Neoproterozoic orogeny, Gondwana Research, 2019, 75, 184-217.	3.0	56

#	Article	IF	CITATIONS
19	Gold endowment in the evolution of the Allaqi-Heiani suture, Egypt: A synthesis of geological, structural, and space-borne imagery data. Ore Geology Reviews, 2019, 110, 102938.	1.1	20
20	Use ofÂLandsat-8 OLI data for delineating fracture systems in subsoil regions: implications for groundwater prospection in the Waddai area, eastern Chad. Arabian Journal of Geosciences, 2019, 12, 1.	0.6	13
21	Gold Metallogeny of the Egyptian South Eastern Desert. Advances in Science, Technology and Innovation, 2019, , 261-263.	0.2	Ο
22	Landsat-8, Advanced Spaceborne Thermal Emission and Reflection Radiometer, and WorldView-3 Multispectral Satellite Imagery for Prospecting Copper-Gold Mineralization in the Northeastern Inglefield Mobile Belt (IMB), Northwest Greenland. Remote Sensing, 2019, 11, 2430.	1.8	72
23	Orogenic gold formation in an evolving, decompressing hydrothermal system: Genesis of the Samut gold deposit, Eastern Desert, Egypt. Ore Geology Reviews, 2019, 105, 236-257.	1.1	25
24	Ediacaran (~ 600 Ma) orogenic gold in Egypt: age of the Atalla gold mineralization and its geological significance. International Geology Review, 2019, 61, 779-794.	1.1	27
25	Trace elements and isotope data of the Um Garayat gold deposit, Wadi Allaqi district, Egypt. Mineralium Deposita, 2019, 54, 101-116.	1.7	11
26	REE geochemical characteristics and satellite-based mapping of hydrothermal alteration in Atud gold deposit, Egypt. Journal of African Earth Sciences, 2018, 145, 317-330.	0.9	31
27	Auriferous shear zones in the central Allaqi-Heiani belt: Orogenic gold in post-accretionary structures, SE Egypt. Journal of African Earth Sciences, 2018, 146, 118-131.	0.9	30
28	Petrogenesis and evolution of the Nuweibi rare-metal granite, Central Eastern Desert, Egypt. Arabian Journal of Geosciences, 2018, 11, 1.	0.6	13
29	Iron oxide copper-gold (IOCG) mineralization at the Imiter inlier, Eastern Anti-Atlas, Morocco. Chemie Der Erde, 2018, 78, 462-478.	0.8	2
30	Application of Multi-Sensor Satellite Data for Exploration of Zn–Pb Sulfide Mineralization in the Franklinian Basin, North Greenland. Remote Sensing, 2018, 10, 1186.	1.8	92
31	Granitoid-associated gold mineralization in Egypt: a case study from the Atalla mine. Mineralium Deposita, 2018, 53, 701-720.	1.7	18
32	Gold-bearing volcanogenic massive sulfides and orogenic-gold deposits in the Nubian Shield. South African Journal of Geology, 2017, 120, 63-76.	0.6	50
33	Mapping the Dyke Swarms of the Eastern Desert, Egypt. Acta Geologica Sinica, 2016, 90, 28-28.	0.8	1
34	Satellite imagery and airborne geophysics for geologic mapping of the Edembo area, Eastern Hoggar (Algerian Sahara). Journal of African Earth Sciences, 2016, 115, 143-158.	0.9	27
35	ASTER-based mapping of ophiolitic rocks: examples from the Allaqi–Heiani suture, SE Egypt. International Geology Review, 2016, 58, 525-539.	1.1	31
36	Lu–Hf and O isotopic compositions on single zircons from the North Eastern Desert of Egypt, Arabian–Nubian Shield: Implications for crustal evolution. Gondwana Research, 2016, 32, 181-192.	3.0	55

BASEM AHMED ZOHEIR

#	Article	IF	CITATIONS
37	Metal and fluid sources in a potential world-class gold deposit: El-Sid mine, Egypt. International Journal of Earth Sciences, 2015, 104, 645-661.	0.9	21
38	Geochemistry and geochronology of the ~620 Ma gold-associated Batouri granitoids, Cameroon. International Geology Review, 2015, 57, 1485-1509.	1.1	38
39	Fluid evolution in the El-Sid gold deposit, Eastern Desert, Egypt. Geological Society Special Publication, 2014, 402, 147-175.	0.8	29
40	Field and ASTER imagery data for the setting of gold mineralization in Western Allaqi–Heiani belt, Egypt: A case study from the Haimur deposit. Journal of African Earth Sciences, 2014, 99, 150-164.	0.9	49
41	Greenstone-hosted lode-gold mineralization at Dungash mine, Eastern Desert, Egypt. Journal of African Earth Sciences, 2014, 99, 165-187.	0.9	29
42	Geochemistry and mineral chemistry of lode gold mineralisation, SE Egypt: implications for ore genesis and exploration. Arabian Journal of Geosciences, 2013, 6, 4635-4646.	0.6	7
43	Au and Cr mobilization through metasomatism: Microchemical evidence from ore-bearing listvenite, South Eastern Desert of Egypt. Journal of Geochemical Exploration, 2013, 125, 34-45.	1.5	32
44	Lode-gold mineralization in convergent wrench structures: Examples from South Eastern Desert, Egypt. Journal of Geochemical Exploration, 2012, 114, 82-97.	1.5	25
45	Controls on lode gold mineralization, Romite deposit, South Eastern Desert, Egypt. Geoscience Frontiers, 2012, 3, 571-585.	4.3	21
46	Integrating geologic and satellite imagery data for high-resolution mapping and gold exploration targets in the South Eastern Desert, Egypt. Journal of African Earth Sciences, 2012, 66-67, 22-34.	0.9	82
47	Microchemistry and stable isotope systematics of gold mineralization in a gabbro–diorite complex, SE Egypt. Microchemical Journal, 2012, 103, 148-157.	2.3	11
48	Transpressional zones in ophiolitic mélange terranes: Potential exploration targets for gold in the South Eastern Desert, Egypt. Journal of Geochemical Exploration, 2011, 111, 23-38.	1.5	49
49	Listvenite–lode association at the Barramiya gold mine, Eastern Desert, Egypt. Ore Geology Reviews, 2011, 39, 101-115.	1.1	91
50	Genesis of the Abu Marawat gold deposit, central Eastern Desert of Egypt. Journal of African Earth Sciences, 2010, 57, 306-320.	0.9	30
51	Epigenetic BIF-hosted gold lodes at the Abu Marawat area, Eastern Desert, Egypt: integrated mineralogical, structural control and fluid inclusion studies. Transactions of the Institution of Mining and Metallurgy Section B-Applied Earth Science, 2009, 118, 59-76.	0.8	2
52	Characteristics and genesis of shear zone-related gold mineralization in Egypt: A case study from the Um El Tuyor mine, south Eastern Desert. Ore Geology Reviews, 2008, 34, 445-470.	1.1	52
53	Role of fluid mixing and wallrock sulfidation in gold mineralization at the Semna mine area, central Eastern Desert of Egypt: Evidence from hydrothermal alteration, fluid inclusions and stable isotope data. Ore Geology Reviews, 2008, 34, 580-596.	1.1	30
54	Structural controls, temperature–pressure conditions and fluid evolution of orogenic gold mineralisation at the Betam mine, south Eastern Desert, Egypt. Mineralium Deposita, 2008, 43, 79-95.	1.7	35

#	Article	IF	CITATIONS
55	Origin and Evolution of the Um Egat and Dungash Orogenic Gold Deposits, Egyptian Eastern Desert: Evidence from Fluid Inclusions in Quartz. Economic Geology, 2008, 103, 405-424.	1.8	51
56	The tectono-metamorphic evolution of the central part of the Neoproterozoic Allaqi–Heiani suture, south Eastern Desert of Egypt. Gondwana Research, 2007, 12, 289-304.	3.0	52